sustainability

MDPI

Article

Revenue Analysis of Stationary and Transportable Battery Storage for Power Systems: A Market Participant Perspective

Zhongyang Zhao, Caisheng Wang * and Masoud H. Nazari

Department of Electrical and Computer Engineering, Wayne State University, Detroit, MI 48202, USA; zhongyang.zhao@wayne.edu (Z.Z.); masoud.nazari@wayne.edu (M.H.N.)
* Correspondence: cwang@wayne.edu

Abstract: The power system faces a growing need for increased transmission capacity and reliability with the rising integration of renewable energy resources. To tackle this challenge, Battery Energy Storage Systems (BESSs) prove effective in enhancing grid capacity and relieving transmission congestion. This paper focuses on the PJM market, conducting a thorough revenue analysis to identify and characterize highly profitable nodes for BESS market participants. A comparison between stationary and transportable BESSs reveals that the transportable BESSs can generate higher potential revenue in energy and regulation markets. Based on these findings, we propose an optimal placement algorithm to support market participants in selecting strategic sites for BESS installation, validated with real PJM market data. This paper provides valuable insights for navigating market-based power system participants and promoting the effective integration of BESSs.

Keywords: battery energy storage system; revenue analysis; optimal placement algorithm; transportable energy storage

check for updates

Citation: Zhao, Z.; Wang, C.; Nazari, M.H. Revenue Analysis of Stationary and Transportable Battery Storage for Power Systems: A Market Participant Perspective. *Sustainability* **2024**, *16*, 2370. https://doi.org/10.3390/su16062370

Academic Editor: Andrea Nicolini

Received: 16 January 2024
Revised: 6 March 2024
Accepted: 6 March 2024
Published: 13 March 2024

Copyright: © 2024 by the authors. Licensee MDPI, Basel, Switzerland. This article is an open access article distributed under the terms and conditions of the Creative Commons Attribution (CC BY) license (https://creativecommons.org/licenses/by/4.0/).

1. Introduction

Facing the challenges of the climate crisis, several states in the U.S. have announced their targets to achieve net-zero emissions by 2050 [1]. As the electric power sector shares 33% of carbon dioxide emissions in the U.S., the emission reduction of the power generation holds the key to reaching net-zero emissions [2]. Using renewable energy resources helps to reduce greenhouse gas emissions, since 2018, the generation capacity of wind and solar has increased by over 30% and 65%, respectively. However, the integration of renewable generation has challenged the operation of power systems. Due to a lack of transmission capacity, the renewable generation has caused transmission congestion and needs to be significantly curtailed [3–5]. Furthermore, numbers of renewable energy projects have to be withdrawn from the interconnection queue in some highly congested regions [6], while building the transmission lines is costly.

Under this situation, the role of battery energy storage systems (BESSs) becomes more and more important as they have the advantages of (1) providing a variety of functions [7], including energy arbitrage, ancillary services, generation, capacity deferral, ramping, congestion relief and accommodation of intermittent renewable energy; (2) enhancing power system resilience and defending against the adversarial attack [8]; and (3) providing more opportunities for small market participants to participate in the market [9]. While BESSs offer substantial benefits for power system resilience and facilitate broader market participation, there are challenges such as (1) the high costs associated with battery technologies and operations and (2) the limited portability of most BESSs remain significant barriers. These aspects underscore the need for continued innovation and policy support to improve the economic viability and flexibility of BESSs.

To benefit the operations of power systems from the implementation of BESS, the Federal Energy Regulatory Commission (FERC) has issued Orders 755 [10] and 841 [9] in 2011 and 2018, respectively, which have further paved the way for market participation of

energy storage. Order 755, titled "Frequency Regulation Compensation in the Organized Wholesale Power Markets", requires the Independent System Operators (ISOs) and Regional Transmission Organizations (RTOs) to pay for the capacity offers and regulation performances provided by energy storage. Order 841, called "Electric Storage Participant in Markets Operated by Regional Transmission Organizations and Independent System Operators", guides ISOs and RTOs toward lowering the barriers for the participation of electric storage resources in the capacity, energy, and ancillary service markets [9]. As the battery technologies advance and the cost of batteries decreases, BESSs have emerged as one of the popular and cost-effective energy storage technologies for power system applications. Recently, the utility-scale BESS applications have experienced exponential growth worldwide. For example, the BESS capacity in the U.S. has increased from 845 MW in 2018 to 14,060 MW in 2023 [11].

In addition, the integration of renewable energy sources has caused serious transmission congestion in the power markets, which makes the Locational Marginal Prices (LMPs) more volatile in the congested regions. The increasing arbitrage opportunities will encourage more BESSs to participate in the wholesale market. Meanwhile, BESSs can also quickly respond to the system control signals, provide mobile and highly flexible storage capacity, and can be placed at desirable locations in the grid for optimal operations, which may improve the power system reliability and better address the energy crisis in the future. Building upon the data analysis and innovative methodologies [12], this paper delves into the economic viability and operational dynamics of battery storage systems, leveraging innovative frameworks to justify the potential of energy storage solutions in enhancing power market efficiency and sustainability.

However, having access to the wholesale market and new profit opportunities does not mean we need to arbitrarily build more BESS projects to dive into the market, while many factors can influence the profits. Due to the volatility and variations in LMP, Regulation Market Clearing Price (MCP), and automatic generation control (AGC) regulation signal of different locations and seasons in the power market, the investment return for market participants can be vastly different. A poor selection of installation location for a BESS can cause it to struggle. Therefore, a comprehensive analysis for finding the locations with the best potential revenues and mitigate the transmission congestion in the wholesale markets is a high-priority task for the market participants who plan to invest in BESS. To analyze the potential income of BESS in the energy and regulation markets, several studies have been carried out [13–20]. The energy storage technologies, potential applications, and comparison of policies on the participation of BESS in different markets were investigated and studied in [13–15]. The analyses of potential revenues have been carried out in MISO [16], PJM [17], CAISO [19], ERCOT [18], and New York ISO [20]. Although the potential revenues of BESS in energy and frequency regulation markets were estimated in [16,17], the estimations were only based on a single node, such as IPL.16STOU6O6 in MISO [16] and HAZLETON 1–4 in PJM [17]. In [18], the possible revenues for BESS were estimated only for the load zones of ERCOT. Because of the insufficient study from the perspective of the whole system, the characteristics of the potential revenues throughout the entire power market have not been revealed for the BESS participants yet.

In addition to the stationary system, BESS can be installed on a mobile platform such as a truck or an aggregation of EVs with Vehicle-to-Grid (V2G) capability. While a transportable BESS can be implemented at different locations during operation, it is also imperative for the market participants to have an estimation on the current and future status of the power market and deploy the BESS at the appropriate site to better accommodate the renewable energy resources and transmission congestion. Therefore, in addition to the temporal system-wide revenue estimation, it is beneficial to optimally locate the portable BESSs to maximize their profitability. However, most of the existing studies on portable BESSs focus on the operation of power systems for the system operator, such as load shifting [21,22], transmission congestion relief [23,24], enhancing the resilience of distribution system [25,26], and the reduction of wind curtailment [27]. An optimal

placement algorithm to maximize revenue in energy and frequency regulation markets from the perspective of a market participant has not been fully investigated yet.

An extensive review of the literature reveals that revenue analysis in existing studies is often limited to individual nodes, lacking a holistic view of the entire power system. Moreover, the role of transportable batteries is typically discussed only in the context of reducing congestion and improving system resilience, leaving a critical gap in the comprehensive revenue analysis for both stationary and transportable BESSs across the entire power market. This area remains underexplored. This paper seeks to fill this gap by providing a detailed revenue analysis of BESSs across the entire power market. Aiming to revolutionize BESS deployment strategies, this paper also introduces an innovative optimal placement algorithm derived from an exhaustive revenue analysis of the entire system and validated with real-world market data. This work is set to enable more strategic and informed decision-making for market participants in BESSs deployment. Therefore, the main contributions of this paper can be summarized as follows:

- **Revenue Estimation and Characterization:** Considering LMPs, regulation MCP and AGC signals, and battery degradation, the potential revenues for BESSs to participate in both the energy and regulation markets are estimated for every node, and the features of nodal profit differences are characterized.
- **Temporal and Spatial Revenue Analysis:** The temporal and spatial revenue analysis is performed by considering transportable BESSs to grasp more profitable opportunities.
- **Optimal Placement Algorithm:** According to the characteristics discovered at the most profitable node, an optimal placement algorithm is proposed for market participants to find the profitable locations for better installation and operation of the BESS, particularly when it is transportable.

The rest of this paper is organized as follows: Section 2 introduces the participation models for estimating the potential revenues of BESS in energy and regulation markets. Section 3 provides the numerical results and detailed revenue analysis of different cases. An optimal placement algorithm of transportable BESSs is proposed in Section 4. The conclusion is drawn in Section 5. Future work is discussed in Section 6.

2. Participation Models in Energy and Frequency Regulation Markets

The following models for participating in PJM energy and frequency regulation markets are used to estimate the potential profit at each commercial pricing node (CPN), which is valid for auction. It is worth noting that, unlike the system operator, the market participants do not have sufficient data to run an accurate DC optimal power flow [28] for the large-scale power market. Hence, the available data for market participants, such as price and regulation signals, are used in the following models for their decisions.

2.1. Credit in Energy Market

The arbitrage credit of energy storage from the energy market during a period of time T is calculated by (1). The time interval is assumed to be one hour.

$$Credit_E = \sum_{t=1}^{T} P_t^{E,dis} \times LMP_t - \sum_{t=1}^{T} P_t^{E,ch} \times LMP_t, \quad (1)$$

where $P_t^{E,ch}$ and $P_t^{E,dis}$ represent the charging and discharging power in the energy market at hour t, and LMP_t is the LMP at hour t.

2.2. Credit in Regulation Market

In addition to the energy market, energy storage can participate in the regulation market. Since this study focuses on analyzing the electric storage projects competing in PJM, the credit calculation method of participating in the frequency regulation market follows the PJM's rules. According to the section about regulation credits in the PJM

manual [29], the regulation remuneration is obtained from two parts, capability and performance, as shown in (2).

$$Credit_R = Credit_{cap} + Credit_{perf} \tag{2}$$

Given an offered capacity P_t^R, Regulation Market Capability Clearing Price $RMCCP_t$, and performance score ρ_t, the $Credit_{cap}$ can be calculated by (3). The performance score ρ_t is used to evaluate how well the resource is following the regulation signal [30].

$$Credit_{cap} = \sum_{t=1}^{T} P_t^R \times RMCCP_t \times \rho_t \tag{3}$$

In PJM's frequency regulation market, there are two types of regulation signals generated every two seconds. One is the Regulation D signal ($RegD$), which is a fast and dynamic signal for fast-responding resources such as BESS. The other one is the Regulation A signal ($RegA$), a slower signal for conventional resources like hydropower [30].

To show the difference between these two signals, a series of 40-min PJM regulation test signals [31] is plotted in Figure 1. According to the plots, $RegD$ has a much higher volatility than $RegA$. The $RegA$ resources typically do not have a duration limit, while the $RegD$ resources are expected to have a short period duration [32]. Hence, the BESS is only considered to submit the offer to follow $RegD$. In the frequency regulation market, the performance credit $Credit_{perf}$ is calculated by (4). In the equation, $RMPCP_t$ is the Regulation Market Performance Clearing Price at hour t, and the Mileage Ratio β_t of $RegD$ over $RegA$ can be obtained by (5). The mileage of a regulation signal indicates the total movements of that signal in a given interval. The mileages of $RegD$ and $RegA$ ($Mileage_t^{RegD}$ and $Mileage_t^{RegA}$) are given in (6) and (7), respectively. n in those two equations is the number of time intervals. For example, to calculate the mileage of a 2 s signal in one hour, n is 1800.

$$Credit_{perf} = \sum_{t=1}^{T} P_t^R \times RMPCP_t \times \beta_t \times \rho_t \tag{4}$$

$$\beta_t = Mileage_t^{RegD} / Mileage_t^{RegA} \tag{5}$$

$$Mileage_t^{RegD} = \sum_{i=0}^{n} \left| RegD_i - RegD_{i-1} \right| \tag{6}$$

$$Mileage_t^{RegA} = \sum_{i=0}^{n} \left| RegA_i - RegA_{i-1} \right| \tag{7}$$

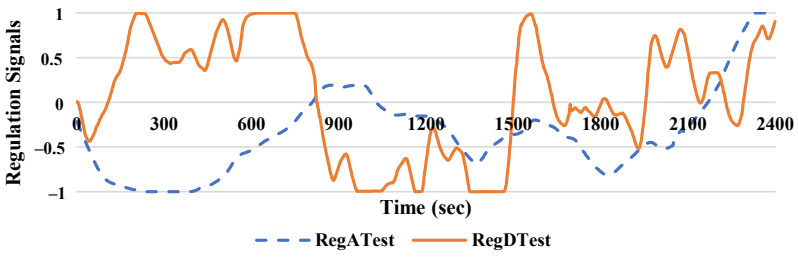


Figure 1. Comparison between $RegA$ and $RegD$.

2.3. Cost of Storage Degradation

Based on [33,34], the degradation cost of BESS is assumed to be a linear function of the BESS output as given in (8) and (9) as follows:

$$Cost_D = \sum_{t=1}^{24} (P_t^{ch} \times \eta_c + P_t^{dis} \times \eta_d^{-1}) \times DEG_{rate} \tag{8}$$

$$DEG_{rate} = (v \times \pi_{ES} \times 0.5) / (1 - \sigma_{EOL}) \tag{9}$$

where P_t^{ch} and P_t^{dis} are the overall charging and discharging power at hour t, respectively; the η_c and η_d are the corresponding charging and discharging efficiency of BESS; DEG_{rate} represents the cost of each MWh charge/discharge of the BESS; υ represents the degradation speed of energy storage; π_{ES} stands for the cost of energy storage; and σ_{EOL} means the storage state at the end of life (EOL).

2.4. Participation of Energy Market

When the BESS only participates in the energy market, the objective of energy arbitrage is to maximize the revenue, as shown in (10). We assume that the forecast of the next day electricity price is accurate, and the participation model is expected to be price-taking. Therefore, the model for participating in the energy market can be described as follows:

$$Max(Credit_E - Cost_D) \tag{10}$$

s.t. (1), (8), (9) and (11)–(18).

$$P_t^{ch} = P_t^{E,ch} \tag{11}$$

$$P_t^{dis} = P_t^{E,dis} \tag{12}$$

$$0 \le P_t^{E,ch} \le P_{max} \tag{13}$$

$$0 \le P_t^{E,dis} \le P_{max} \tag{14}$$

$$P_t^{E,ch} \times P_t^{E,dis} = 0 \tag{15}$$

$$0 \le S_t \le 100\% \tag{16}$$

$$S_t = S_{t-1} + (P_t^{ch} \times \eta_c - P_t^{dis} \times \eta_d^{-1})/E_{max} \times 100\% \tag{17}$$

$$S_0 = S_{24} \tag{18}$$

where the P_t^{ch} and P_t^{dis} are determined by (11) and (12). P_{max} and E_{max} are the power rating and energy capacity of the BESS. S_t represents the state of charge (SOC) at time t. The operation limits of the BESS are set by (13)–(16). S_0 and S_{24} are the SOC at $t = 0$ and $t = 24$ of each day. S_t is obtained from the previous SOC S_{t-1} and the hourly output, as given in (17). Equation (18) is implemented to ensure that the conditions of daily optimization are consistent. Equation (15) is used to force the optimization model to not make charging and discharging offers at the same time. Furthermore, (15) is essential for the market participation model to deal with negative LMPs.

2.5. Participation of Energy and Frequency Regulation Markets

When the BESS participates in the energy and frequency regulation markets simultaneously, the objective function is formulated by (19) to achieve the maximum daily profit at a node.

$$Max(Credit_E + Credit_R - Cost_D) \tag{19}$$

s.t. (1)–(9), (13)–(18) and (20)–(24).

The P_t^{ch} and P_t^{dis} of the degradation cost for both the energy and regulation markets are calculated by (20) and (21), where $RegD_t^{up}$ and $RegD_t^{down}$ are the absolute values of hourly accumulations of the regulation up and down signals. In PJM, a unit offering in the

regulation market is required to be able to provide the same amount of positive capacity and negative capacity. The constraints of output offers are given in (22)–(24).

$$P_t^{ch} = P_t^{E,ch} + P_t^R \times RegD_t^{down} \tag{20}$$

$$P_t^{dis} = P_t^{E,dis} + P_t^R \times RegD_t^{up} \tag{21}$$

$$0 \le P_t^R \le P_{max} \tag{22}$$

$$0 \le P_t^{E,ch} + P_t^R \le P_{max} \tag{23}$$

$$0 \le P_t^{E,dis} + P_t^R \le P_{max} \tag{24}$$

Implementing the introduced participation models with the real market data, such as LMP, RMCCP, RMPCP, and *RegD*, the maximum daily revenue at each node can be obtained and the nodes with the best profitability can be identified, as discussed in Section 3.

3. Revenue Analysis of BESSs

3.1. Data Preparation

There are over 12,000 pricing nodes in PJM, and about 7000 of them are valid for auction [35]. This paper focuses on analyzing the potential revenue of BESS at the valid nodes. According to the market participation models, introduced in Section 2, the LMP, AGC regulation signals, regulation mileage, RMCCP, and RMPCP are required for estimating the potential revenue of participating in the energy and regulation markets. In this paper, the corresponding 12-month market data in 2018 are collected via PJM Data Miner 2 [36], which is a data management tool to access PJM data. The potential profit of transportable BESS is investigated in different seasons [37]. In the energy market, LMP reflects the value of electricity at different nodes, which is defined as the cost of supplying the next 1 MW at the node [38]. LMP is a combination of three components: price of energy, power system congestion, and energy loss. Since these components are affected by load, fuel cost, system topology, etc., the LMPs can have different characteristics and values at different periods and locations, which can cause significant changes in the BESS revenue. Unlike the energy market, the regulation market is pool-based, which implies that there is only one market clearing price for each MW supplied. Hence, all resource owners are credited by the same price for providing the scheduled regulation output. To calculate the potential profit of participating in the regulation market, the hourly LMP, RMCCP, RMPCP, *RegA* mileage, and *RegD* mileage in 2018 are collected. To determine the hourly regulation output and the hourly SOC, the 2 s regulation signals [39] are also collected and aggregated to the hourly regulation up and down signals. In this paper, we study the revenue maximization of a 10 MW/10 MWh BESS. The BESS can achieve charge/discharge (η_c/η_d) efficiency at 95%. To estimate the degradation cost, the degradation speed of energy storage υ, the cost of energy storage π_{ES}, and the storage state at the end of life σ_{EOL} are set at 3×10^{-5}, 1×10^5 \$/MWh, and 0.8, respectively, [33,34]. In this study, the initial SOC S_0 of each day is set to be 50%. Given these BESS parameters, the degradation rate DEG_{rate} in (9) can be obtained as 7.5 \$/MWh. This degradation cost indicates that the charging action is worthless for the battery when the profit of 1 MWh charge cycle is less than \$15.

3.2. Potential Revenue of Stationary BESS

The first case study is to place the BESS at one location for an entire year (1L1Y), which is the most common setup investigated in the previous studies [13,15–20,40–42]. The proposed optimal placement algorithm finds a profitable location in the system to build the BESS and obtains the credit settled by the corresponding LMP and regulation MCP for a long period. The 1L1Y utilizes the real market data, including the RTLMP, RMCCP, RMPCP, and the regulation signal, to estimate the potential annual revenues at different settlement price nodes in PJM, which provides the valuable information for implementing BESS from the perspective of market participants. Given the 2018 market data collected

from PJM, the maximum potential revenue and the corresponding generation outputs of each node can be obtained by the participation models proposed in Section 2. As shown in Figure 2, the percentiles of all nodes' potential revenues are grouped and mapped into five different colors, which indicate the percentiles of 0–20%, 20–40%, 40–60%, 60–80%, and 80–100%, respectively. The percentile indicates the revenue's percentage rank of a specified node among all nodes. According to the revenue distribution, the nodes of the top 20% (i.e., 80–100%) annual revenues are found to concentrate in some regions. In other words, the nodes which have high potential revenue for stationary BESS are not randomly distributed in the power market. It is feasible for market participants to locate some sites to enhance their competitiveness in the power market. In addition, Figure 2 clearly indicates that there is a sharp increase in revenue for the nodes falling in the 80–100% percentile interval. Notably, the annual revenue at the most lucrative node, named ROCKWLKN69KV LS-EGRET (ROCK), is \$2.7 M, which is \$530 k higher than the annual revenue at the least lucrative node, called 21 KINCA20KV KN-1 (KINCA). In other words, the BESS at ROCK could earn 23.5% more profit than the BESS at KINCA in 2018.

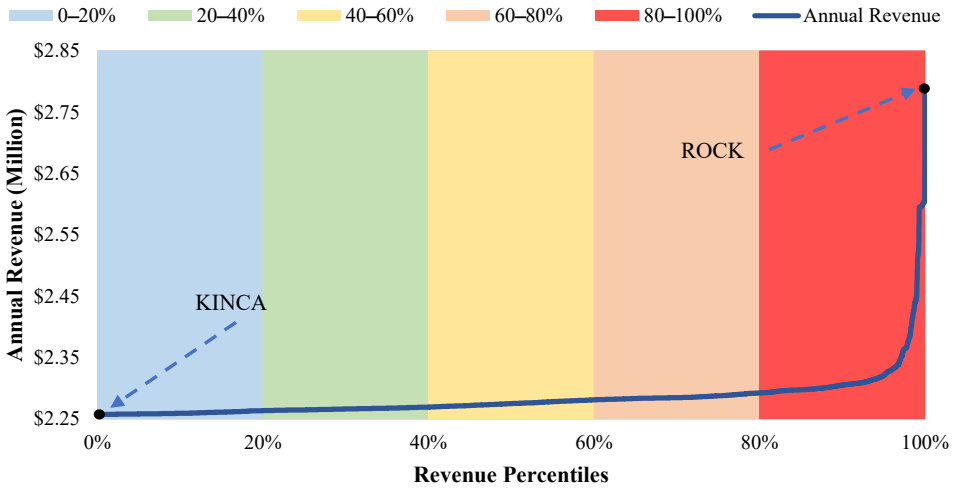


Figure 2. Annual revenues by percentiles.

To gain a more comprehensive understanding of the factors causing the revenue disparity, the differences in daily revenues in 2018 between these two nodes are calculated and plotted in Figure 3. It can be seen that most of the daily revenue differences are low, and the significant revenue differences are in May, October, and November.

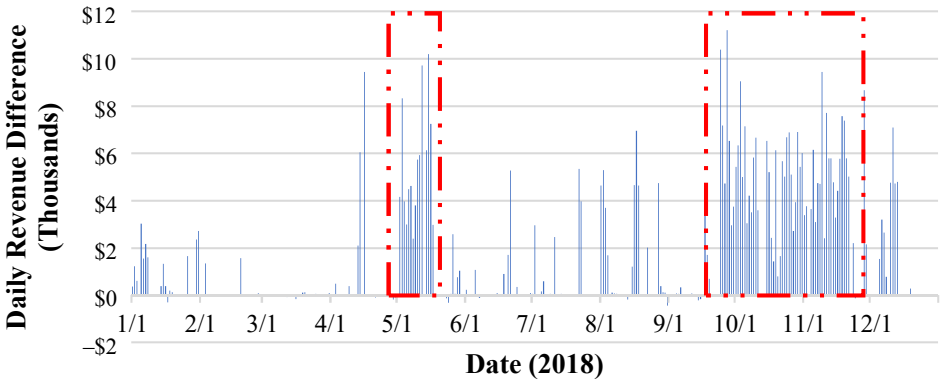


Figure 3. Daily revenue differences between ROCK and KINCA in 2018.

Moreover, when the daily revenue differences are sorted into ascending order, the accumulation of the sorted daily revenue differences can be obtained and plotted in Figure 4. The x-axis indicates the percentiles of the daily revenue differences, and the

y-axis shows the accumulated revenue difference over the sorted daily revenue difference. According to the accumulated revenue difference shown in Figure 4, 80% of the total annual revenue difference is found to be contributed by the top 19.45% of the daily revenue difference. This means the potential profit at node ROCK does not overwhelm the potential profit at node KINCA on every single day. Most of the annual revenue difference is just accumulated in a short period.

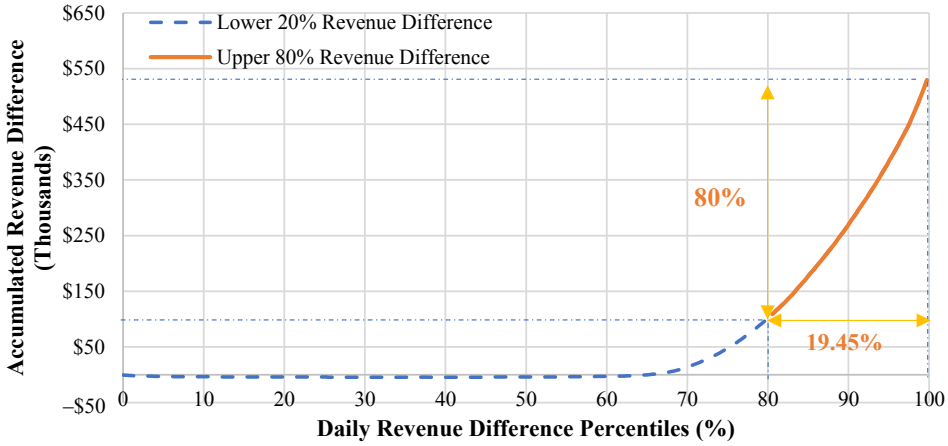


Figure 4. Accumulation of sorted revenue difference.

Furthermore, to obtain more details about the revenue difference, the hourly LMPs of KINCA and ROCK nodes on the days of the top 19.45% daily revenue differences are extracted. The boxplots of the extracted 24-h LMPs in Figure 5 shows the hourly LMPs at ROCK have a much higher volatility than the LMPs at KINCA. At node ROCK, the LMPs from 6:00 a.m. to 9:00 a.m. and from 1:00 p.m. to 11:00 p.m. are distributed on a larger price range than the other hours, which enables the BESS to have more arbitrage opportunities in the energy market. Notably, a large amount of negative prices are found at node ROCK, and the negative rates make the charging action profitable.

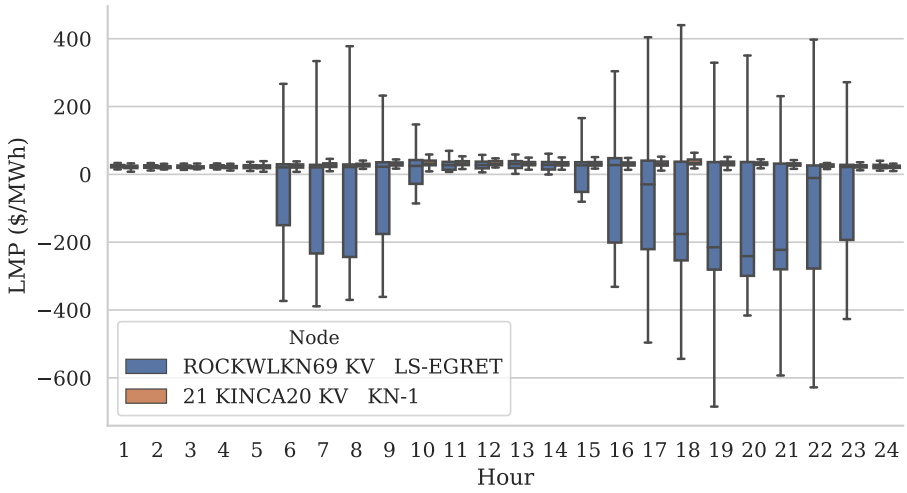


Figure 5. LMP features of the top 20% of daily revenue differences.

According to the optimization results on 27 September 2018, the battery at node ROCK can earn $17 k, while the battery at node KINCA can just earn $5.9 k. There is $11 k revenue difference, which is more than 189% of the daily revenue at node KINCA on 27 September 2018. This is the most significant difference in daily revenue between these two nodes in 2018. To better illustrate the BESS behavior, their optimized generation outputs on 27 September 2018 are extracted and displayed in Figures 6 and 7. Given the

optimized outputs, their hourly SOCs on 27 September 2018 can be calculated by (17). As a reference, the corresponding hourly state of energy (SOE) derived from SOC is plotted with the LMPs in Figures 6 and 7.

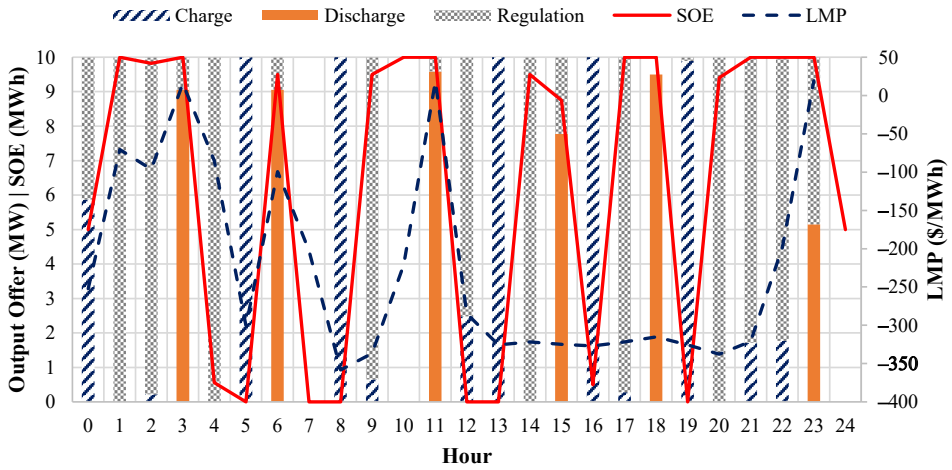


Figure 6. Output actions of node ROCK on 27 September 2018.

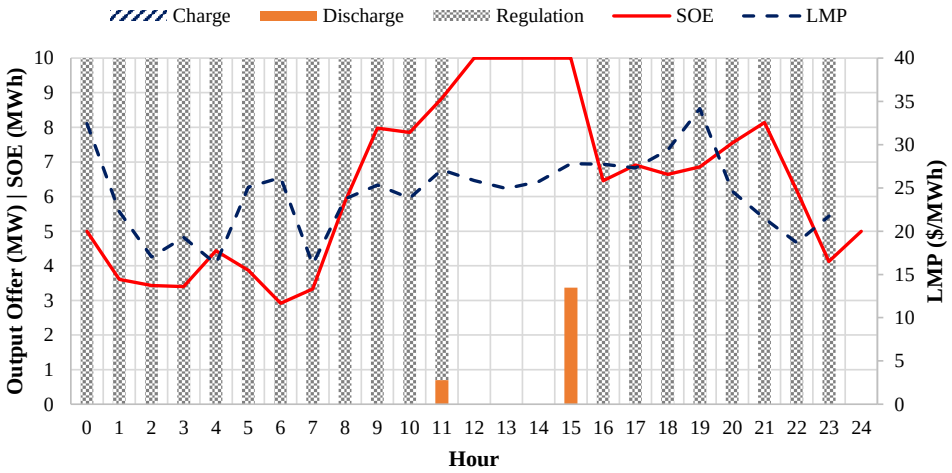


Figure 7. Output actions of node KINCA on 27 September 2018.

In Figures 6 and 7, the left y-axis indicates the hourly output power and the SOE of the BESS. The y-axis on the right shows the LMP at the node. The bars of different colors at each hour display charging power, discharging power, and regulation output, respectively. The solid and dash lines show the hourly SOEs and LMPs in 24 h. As shown in Figure 6, the LMP at node ROCK is very volatile, and the peak prices on 27 September 2018 happen at 3:00 a.m., 6:00 a.m., 11:00 a.m., and 11:00 p.m., when the discharging actions are taken for arbitraging in the energy market. When the LMPs are low, the charging actions are found at 5:00 a.m., 8:00 a.m., 1:00 p.m., and 7:00 p.m.

In Figure 7, the standard deviation of 24-h LMPs is $4.67/MWh. Compared to the LMPs in Figure 6 with $128.11/MWh standard deviation, the LMPs at KINCA are less volatile, which indicates fewer arbitrage opportunities. In addition, the degradation cost, implemented in the market participation models, forces the BESS not to charge or discharge any single MWh when the arbitrage revenue cannot cover the degradation cost. Due to the degradation cost, it can be seen in Figure 7 that most of the output power at node KINCA is offered to the regulation market. From 12:00 to 15:00, the BESS at KINCA does not even provide full output capacity since the earnings from energy and regulation markets during these hours are not able to cover the degradation cost. Comparing the discharging actions at node KINCA to the multiple charging and discharging actions at node ROCK, the factor

that leads to an $11 k daily revenue difference on 27 September 2018 can be discovered. It is the volatility of LMP at node ROCK which makes the BESS produce more revenue. As mentioned earlier, the LMP is a combination of three components. Since there is only one energy price for all the buses in the system and the energy loss is relatively small compared to the other components [38], the power system congestion becomes the dominating factor that influences the potential revenue for the BESS, participating in the energy and regulation markets. In other words, to achieve more revenue, the BESS should search for a place with a highly volatile congestion component. An interesting point that can be observed in Figure 7 is the advantage of participating in both the energy and regulation markets. According to the optimization results, the battery at node KINCA can still make $5.9 k profit on 27 September 2018, which means that the BESS can always guarantee a certain amount of profit by participating in the regulation market even though there is a lack of arbitrage opportunity in the energy market.

3.3. Potential Revenue of Transportable BESS

Recalling from the previous section, a significant part of the annual revenue difference is accumulated in a short period. Meanwhile, the renewable energy resources have a strong seasonal pattern [43]. Thus, if the BESS is on a transportable platform (such as trucks) that can be installed and commissioned at different places in different seasons or months, it can capture more revenue in the market and better accommodate the renewable energy resources and transmission congestion. A transportable BESS can also be formed by aggregating a fleet of EVs that have the V2G capabilities. To study the potential revenue of the transportable BESS, the cases of settling the BESS at 4 Locations in 4 Seasons (4L4S) and 12 Locations in 12 Months (12L12M) are studied in the following. Based on the annual motor carrier operations cost report [44] provided by the American Transportation Research Institute (ATRI), the average carrier cost, including driver costs, fuel, insurance, permits, tolls, etc., is set to $66.65/h. Similar to [24], the size of BESS on each truck is assumed to be 2.5 MW/2.5 MWh. Therefore, the 10 MW/10 MWh BESS analyzed can be carried by four trucks. The maximum transportation distance in PJM is expected to be 900 miles, which can cover the distance from Chicago, IL, to Virginia Beach, VA. The average speed of the truck is assumed to be 60 miles/h, so the maximum transportation time is about 15 h, and the transportation cost is $4 k. In addition to the cost during transportation, it is assumed that the wage of a professional electrician is $65/h and the integration work will take 10 electricians 4 h to complete. Then the labor cost for integration is estimated at $3 k, including the electrician cost, insurance, etc. Meanwhile, according to the PJM transmission tariff [45,46], the cost for transmission interconnection of a 10 MW/10 MWh BESS is assumed to be $2.2 k, which includes the costs for the application, feasibility study, and non-refundable deposit. Hence, the maximum cost for each re-location of the 10 MW/10 MWh BESS is $9.2 k. It should be noted that the above re-location cost does not apply to a virtual transportable BESS, consisting of aggregated EVs.

According to the optimization results, all nodes' daily revenues can be obtained and aggregated to the seasonal revenues. More specifically, the most profitable nodes and their seasonal earnings are obtained based on the daily maximum revenues, as listed in Table 1. As a comparison, the seasonal revenues of 1L1Y are shown in Table 1, as well. The seasonal profits of 4L4S surpass the seasonal profits of 1L1Y by $28 k, $33 k, and $118 k in spring, summer, and winter, respectively. In fall, the nodes with the best potential revenue of 1L1Y and 4L4S are the same. Therefore, if the BESS is transportable, the best possible earning for 4L4S is $2.9 M, which is $180 k higher than the annual revenue at the best fixed location (i.e., node ROCK). Even considering the $37 k transportation cost for 4L4S, the transportable BESS is still more profitable than the stationary BESS in 1L1Y.

Table 1. Seasonal revenues of 1L1Y and 4L4S.

Season	Node	1L1Y Profit	Node	4L4S Profit
Spring	ROCK	\$688 k	STRASBUR	\$716 k
Summer	ROCK	\$489 k	CEDARCRE	\$523 k
Autumn	ROCK	\$769 k	ROCK	\$769 k
Winter	ROCK	\$837 k	GARDNERS	\$955 k

The 12L12M scheme is studied for transportable BESS as well. In the 12L12M case, the BESS are transported every month to maximize the revenue in the energy and regulation markets. According to the monthly revenue listed in Table 2, the potential revenue of 12L12M is \$3.2 M. Even considering the \$110 k transportation cost in a year, the maximum profit of 12L12M is \$177 k higher than the revenue of 4L4S and \$319 k more than the revenue of 1L1Y.

Table 2. Revenues of 12L12M.

Season		**Spring**			**Summer**	
Month	3	4	5	6	7	8
Profit	\$191 k	\$262 k	\$313 k	\$185 k	\$179 k	\$205 k
Season		**Autumn**			**Winter**	
Month	9	10	11	12	1	2
Profit	\$218 k	\$317 k	\$234 k	\$220 k	\$726 k	\$163 k

4. Optimal Placement of BESSs

The previous revenue analysis is based on historical data. However, the most profitable nodes identified using historical data may not be the appropriate locations for BESSs in the future. Hence, an optimization algorithm is needed for placing and operating the BESSs. This algorithm is particularly important for the transportable BESS participants since they can move to different locations for more profitable opportunities. To achieve this goal, an optimal placement algorithm is proposed in this section for market participants. Without loss of generality, the algorithm that aims for the optimal placement for the next month can be extended to other future times, such as the next season or year.

4.1. Prediction of LMP's Volatility

Recalling from the previous section, the revenue difference among the nodes is caused by the volatility of LMP in the energy market. Hence, to identify the most profitable nodes, the prediction of LMP volatility becomes a critical task. Thus, a standard ARIMA model [47], which is effective for forecasting price sequences [48–50], is used. An ARIMA model can be described by (25) [47].

$$\phi_p(B)\nabla^d y_t = \mu + \theta_q(B)\varepsilon_t, \tag{25}$$

where B is the backward shift operator; p is the auto-regression (AR) order, which determines how many past values are used for regression; d is the differencing order, which represents the number of differencing transformations to make the training series stationary; and q is the moving-average (MA) order to determine how many previous error terms ε_t should be considered. The error terms ε_t are independent and identically distributed noise with zero mean and finite variance.

Given the hourly LMP, the monthly standard deviations of LMP at each node can be calculated. For formulating a stationary series for the ARIMA model, the time series $y_{i,t}$ is obtained by a natural logarithm transformation of a differential series, as shown in (26).

$$y_{i,t} = log(\sigma_{i,t} - \sigma_{PJM,t} + c) \tag{26}$$

where $\sigma_{i,t}$ is the standard deviation of LMP at node i in month t; $\sigma_{PJM,t}$ represents the standard deviation of the system's LMP in month t; c is a positive constant offset to guarantee the logarithm transformation; and $y_{i,t}$ is the transformed time series in month t, which is used by the ARIMA model to forecast the LMP volatility at node i. The LMPs from 1 January 2016 to 31 December 2018 of each node are used for training the ARIMA model to predict the corresponding standard deviation in the next month. The market data between 1 January 2019 and 30 June 2019 are used to validate the proposed algorithm.

4.2. Clustering of Pricing Nodes

In addition to the estimation of LMPs' volatility, the clustering of nodes is important for the optimal BESS placement. After grouping the nodes according to the LMPs' features in the past month, the algorithm can place the transportable BESSs at the nodes in different clusters for the purpose of reducing the risk and seeking for more profitable opportunities throughout the market. The K-means [51], one of the most widely used clustering algorithms, is implemented to cluster the nodes into different groups via minimizing the objective function described in (27) as follows:

$$Min(\sum_{k=1}^{K} \sum_{x \in G_k} \|x - \mu_k\|^2) \tag{27}$$

where K is the total number of clusters, which is determined by the elbow method [52]; G_k represents the k-th group of the clustered data x; and μ_k is the mean of x in G_k (also called centroid). The objective of K-means is to minimize the sum of the Euclidean distance between the data points and the centroid of the corresponding group. To address the high-dimensional hourly LMP for K-means clustering, the hourly LMP in the previous month is grouped by each day to obtain the daily standard deviation. Given the daily standard deviations of each node, the Principle Component Analysis (PCA) [53] is implemented to further reduce the dimension of the historical data. The PCA is a linear transformation to represent the original data by a set of orthogonal variables. Via PCA, the original data can be described with a low dimensional subspace with keeping much of the variance in the dataset. x in (27) is the PCA components of normalized daily standard deviation of the LMPs at each node. By implementing the PCA and K-means for the LMPs in the previous month, the clusters of different nodes can be obtained.

4.3. Optimal Placement Algorithm

Given the prediction of LMP's monthly standard deviations and the clusters of nodes, an algorithm shown in (28)–(31) is designed to assist the market participants for optimal placement of BESSs. The objective is to maximize the sum of the predicted LMP's volatility of the selected nodes, as shown in (28).

$$Max(\sum_{i=1}^{N} \delta_i \, \sigma'_{i,t+1}) \tag{28}$$

s.t. (29)–(31).

$$\sum_{i=1}^{N} \delta_i = N_{ES} \tag{29}$$

$$\sum_{i \in G_k} \delta_i \leq \overline{N}_{Clu} \tag{30}$$

$$\delta_i \, \delta_j \, d_{i,j}^{Geo} \geq \underline{D}^{Geo}, \ \ \forall i < j, \tag{31}$$

where $\sigma'_{i,t+1}$ is the forecast monthly standard deviation of the LMPs at node i; δ_i is a binary decision variable. When $\delta_i = 1$, the node i is selected for placing transportable BESS. Equation (29) indicates that the algorithm needs to find N_{ES} locations for placing the BESSs. Equation (30) ensures that no more than $\overline{N}_{Clu}$ BESSs can be placed in cluster G_k. Since the nodes in the same cluster could have similar characteristics of LMPs, Equation (30) enables the market participants to place the BESSs in different clusters for the risk diversification. Equation (31) ensures that the geographical distance $d_{i,j}^{Geo}$ between nodes i and j must be larger than $\underline{D}^{Geo}$. This information is beneficial for the risk management of market participants. When more system information is available to the market participants, the geographical distance can be extended to other types of distance, such as the electrical distance between the nodes. Furthermore, (31) can be transformed to linear constraints as shown in (32)–(34), where $\delta_{i,j}$ is a binary variable, and M is a large positive number. Therefore, the optimal placement algorithm can be solved as the following mixed-integer linear programming problem.

$$\delta_{i,j} \geq \delta_i + \delta_j - 1, \ \ \forall i < j \tag{32}$$

$$\delta_{i,j} \leq \delta_i, \ \delta_{i,j} \leq \delta_j, \ \ \forall i < j \tag{33}$$

$$\delta_{i,j} \, d_{i,j}^{Geo} + (1 - \delta_{i,j}) \, M \geq \underline{D}^{Geo}, \ \ \forall i < j \tag{34}$$

4.4. Performance of the Proposed Algorithm

In order to evaluate the algorithm's performance, we assume that the market participant needs to place 5 10 MW/10 MWh BESSs in the market for the next month, which indicates $N_{ES} = 5$. Meanwhile, $\overline{N}_{Clu}$ is set to 1, which means no more than 1 BESS can be placed in the same cluster of nodes. The minimum distance $\underline{D}^{Geo}$ between two BESSs is chosen to be 50 miles. With the implementation of the proposed optimal placement algorithm for the first 6 months in 2019, the optimal nodes for placing the BESSs in each month can be obtained. For comparison, a base case for placing the BESSs in the market based on the historical revenue is included, where the market participants use the five most profitable nodes in the current month as the placements for the next month. The market data, such as RTLMP, RMCCP, RMPCP, and the regulation signals, from 1 January 2019 to 31 June 2019, are collected to verify the algorithm.

As shown in Table 3, the optimal placement algorithm can outperform the base case in 5 out of 6 months. In the first 5 months, the algorithm can earn 11.4% more revenue than the base case. Even though the base case beats the proposed algorithm by \$117 k in the last month, the optimal placement algorithm can still make \$194 k more profit than the base case. In other words, the optimal placement algorithm is capable of benefiting market participant by identifying the potentially profitable sites to deploy the BESSs.

Table 3. Performances of the base case and the proposed algorithm.

Mo.	Base	Proposed	Mo.	Base	Proposed
1	\$551 k	\$623 k	**4**	\$560 k	\$618 k
2	\$513 k	\$559 k	**5**	\$434 k	\$509 k
3	\$673 k	\$733 k	**6**	\$592 k	\$475 k

5. Conclusions

This paper carried out a comprehensive and system-wide analysis of potential revenues of BESSs in a market-based power system. The PJM market has been used as a case study, and the features of market data of different locations and seasons have been characterized for the analyses. Based on the distributions of BESS revenue, a set of candidate sites have been identified for installing a BESS in the market to achieve the highest revenue.

By contrasting the most and least profitable nodes, we identified LMP volatility as the pivotal factor influencing revenue maximization. Notably, the majority of the annual revenue variance was concentrated within brief periods, highlighting the lucrative prospects of transportable BESSs capable of capturing profits across various locations and time frames. A study of different seasons and months across all system nodes unveiled that a transportable BESS outperforms a stationary counterpart in both energy and regulation markets. In addition to these findings, we developed and validated an algorithm for the optimal placement of BESSs, offering promising guidance to market participants seeking investments in the energy and frequency regulation markets. Simultaneously, the increasing integration of BESSs holds the potential to fortify power systems in adapting to more renewable energy sources. This comprehensive study serves as a valuable resource for BESS market participants, providing insights for informed decision making in dynamic and evolving power markets.

6. Future Work

While this study presents comprehensive insights into the potential and challenges of BESSs in power systems, it also acknowledges existing limitations. Future work will focus on the following:

- **Advanced Deep Learning Models:** The proposed algorithm is based on the traditional data processing model, such as ARIMA and KNN models. Our future research will explore more sophisticated deep learning techniques to enhance the comparison with the proposed method to relocate the transportable BESSs, aiming to further refine the accuracy and efficiency of revenue predictions.
- **Cross-Market Analysis:** To implement the advanced deep learning model and by extending the dataset to encompass various power markets, we intend to robustly validate the effectiveness of the proposed algorithms and deep learning algorithm. This comprehensive analysis will help in understanding the applicability and scalability of our approach.
- **Policy and Regulatory Impact Studies:** Recognizing the dynamic nature of policy and regulation, we are particularly interested in examining a broader range of scenarios. This will involve assessing the impact of diverse policy and regulatory frameworks on the revenue streams of market participants. Through this exploration, we aim to provide actionable insights that can adapt to changing regulatory landscapes, thereby supporting market participants in making informed decisions.

Author Contributions: Z.Z.: Conceptualization, Methodology, Validation, Writing—Original Draft Preparation; C.W.: Supervision, Funding Acquisition, Writing—Reviewing and Editing; M.H.N.: Writing—Reviewing and Editing. All authors have read and agreed to the published version of the manuscript.

Funding: C. Wang and M.H. Nazari's work were partially supported by the Department of Energy, Solar Energy Technologies Office (SETO) Renewables Advancing Community Energy Resilience (RACER) program under Award Number DE-EE0010413. Any opinions, findings, conclusions, or recommendations expressed in this material are those of the authors and do not necessarily reflect the views of the Department of Energy.

Institutional Review Board Statement: Not applicable.

Informed Consent Statement: Not applicable.

Data Availability Statement: The original data presented in the study are openly available in PJM Data Miner 2: Public Data at https://dataminer2.pjm.com/list.

Conflicts of Interest: The authors declare no conflict of interest.

References

1. U.S. State Greenhouse Gas Emissions Targets. Available online: https://www.c2es.org/document/greenhouse-gas-emissions-targets/ (accessed on 1 December 2023).
2. Energy-Related CO_2 Emission Data Tables, Table 4. Available online: https://www.eia.gov/environment/emissions/state/ (accessed on 1 December 2023).
3. Berizzi, A.; Bovo, C.; Ilea, V.; Merlo, M.; Miotti, A.; Zanellini, F. Decentralized congestion mitigation in HV distribution grids with large penetration of renewable generation. *Int. J. Electr. Power Energy Syst.* **2015**, *71*, 51–59. [CrossRef]
4. Schermeyer, H.; Studer, M.; Ruppert, M.; Fichtner, W. Understanding distribution grid congestion caused by electricity generation from renewables. In *Smart Energy Research. At the Crossroads of Engineering, Economics, and Computer Science*; Springer: Cham, Switzerland, 2017; pp. 78–89.
5. VER Curtailments—SPP Marketplace. Available online: https://marketplace.spp.org/pages/ver-curtailments (accessed on 1 October 2023).
6. Sustainable FERC Project: MISO Interconnection Queue. Available online: https://sustainableferc.org/navigating-miso/ (accessed on 1 October 2023).
7. Sioshansi, R.; Denholm, P.; Jenkin, T. Market and policy barriers to deployment of energy storage. *Econ. Energy Environ. Policy* **2012**, *1*, 47–64. [CrossRef]
8. Li, J.; Wang, J.; Chen, L.; Yu, Y. Defending Against Adversarial Attacks by Energy Storage Facility. In Proceedings of the 2022 IEEE Power & Energy Society General Meeting (PESGM), Denver, CO, USA, 17–21 July 2022; pp. 1–5.
9. FERC Order No. 841. Available online: https://www.ferc.gov/media/order-no-841 (accessed on 20 October 2023).
10. FERC Order No. 755. Available online: https://www.ferc.gov/sites/default/files/2020-06/OrderNo.755-A.pdf (accessed on 20 October 2023).
11. Preliminary Monthly Electric Generator Inventory (Based on Form EIA-860M as a Supplement to Form EIA-860). Available online: https://www.eia.gov/electricity/data/eia860m/ (accessed on 20 October 2023).
12. Tian, J.; Shen, C.; Wang, B.; Xia, X.; Zhang, M.; Lin, C.; Li, Q. LESSON: Multi-Label Adversarial False Data Injection Attack for Deep Learning Locational Detection. *IEEE Trans. Dependable Secur. Comput.* **2024**. [CrossRef]
13. Xu, B.; Dvorkin, Y.; Kirschen, D.S.; Silva-Monroy, C.A.; Watson, J.P. A comparison of policies on the participation of storage in us frequency regulation markets. In Proceedings of the 2016 IEEE PES General Meeting, Boston, MA, USA, 17–21 July 2016; pp. 1–5.
14. Wang, Z.; He, Y. Two-stage optimal demand response with battery energy storage systems. *IET Gener. Transm. Distrib.* **2016**, *10*, 1286–1293. [CrossRef]
15. Eyer, J.; Corey, G. Energy storage for the electricity grid: Benefits and market potential assessment guide. *Sandia Natl. Lab.* **2010**, *20*, 5.
16. Nguyen, T.A.; Byrne, R.H.; Concepcion, R.J.; Gyuk, I. Maximizing revenue from electrical energy storage in MISO energy & frequency regulation markets. In Proceedings of the 2017 IEEE PES General Meeting, Chicago, IL, USA, 16–20 July 2017; pp. 1–5.
17. Byrne, R.H.; Concepcion, R.J.; Silva-Monroy, C.A. Estimating potential revenue from electrical energy storage in PJM. In Proceedings of the 2016 IEEE PES General Meeting, Boston, MA, USA, 17–21 July 2016; pp. 1–5.
18. Byrne, R.H.; Silva-Monroy, C.A. Potential revenue from electrical energy storage in ERCOT: The impact of location and recent trends. In Proceedings of the 2015 IEEE PES General Meeting, Denver, CO, USA, 26–30 July 2015; pp. 1–5.
19. Byrne, R.H.; Nguyen, T.A.; Copp, D.A.; Concepcion, R.J.; Chalamala, B.R.; Gyuk, I. Opportunities for energy storage in CAISO: Day-ahead and real-time market arbitrage. In Proceedings of the 2018 International SPEEDAM), Amalfi, Italy, 20–22 June 2018; pp. 63–68.
20. Walawalkar, R.; Apt, J.; Mancini, R. Economics of electric energy storage for energy arbitrage and regulation in New York. *Energy Policy* **2007**, *35*, 2558–2568. [CrossRef]
21. Khodayar, M.E.; Wu, L.; Li, Z. Electric vehicle mobility in transmission-constrained hourly power generation scheduling. *IEEE Trans. Smart Grid* **2013**, *4*, 779–788. [CrossRef]
22. Knezović, K.; Martinenas, S.; Andersen, P.B.; Zecchino, A.; Marinelli, M. Enhancing the role of electric vehicles in the power grid: Field validation of multiple ancillary services. *IEEE Trans. Transport. Electrific* **2016**, *3*, 201–209. [CrossRef]
23. Sun, Y.; Li, Z.; Shahidehpour, M.; Ai, B. Battery-based energy storage transportation for enhancing power system economics and security. *IEEE Trans. Smart Grid* **2015**, *6*, 2395–2402. [CrossRef]
24. He, G.; Zhang, D.; Pi, X.; Chen, Q.; Kar, S.; Whitacre, J. Spatiotemporal Arbitrage of Large-Scale Portable Energy Storage for Grid Congestion Relief. In Proceedings of the 2019 IEEE PES General Meeting, Atlanta, GA, USA, 4–8 August 2019.
25. Yan, X.; Gu, C.; Li, F.; Wang, Z. LMP-based pricing for energy storage in local market to facilitate PV penetration. *IEEE Trans. Power Syst.* **2017**, *33*, 3373–3382. [CrossRef]
26. Yao, S.; Wang, P.; Zhao, T. Transportable energy storage for more resilient distribution systems with multiple microgrids. *IEEE Trans. Smart Grid* **2018**, *10*, 3331–3341. [CrossRef]

27. Sun, Y.; Zhong, J.; Li, Z.; Tian, W.; Shahidehpour, M. Stochastic scheduling of battery-based energy storage transportation system with the penetration of wind power. *IEEE Trans. Sustain. Energy* **2016**, *8*, 135–144. [CrossRef]
28. Frank, S.; Rebennack, S. An introduction to optimal power flow: Theory, formulation, and examples. *IIE Trans.* **2016**, *48*, 1172–1197. [CrossRef]
29. PJM Manual 28: Operating Agreement Accounting. Available online: https://www.pjm.com/~/media/documents/manuals/m28.ashx (accessed on 1 December 2023).
30. PJM Manual 12: Balancing Operations. Available online: https://www.pjm.com/-/media/documents/manuals/m12.ashx (accessed on 1 December 2023).
31. PJM Normalized Regulation Test Signals. Available online: https://www.pjm.com/-/media/markets-ops/ancillary/reg-data-external-may-2014.ashx (accessed on 20 October 2023).
32. PJM Regulation Market: Characteristic Differences Between Resources. Available online: https://learn.pjm.com/three-priorities/buying-and-selling-energy/ancillary-services-market/regulation-market (accessed on 20 February 2024).
33. Wang, Y.; Wan, C.; Zhou, Z.; Zhang, K.; Botterud, A. Improving deployment availability of energy storage with data-driven agc signal models. *IEEE Trans. Power Syst.* **2017**, *33*, 4207–4217. [CrossRef]
34. Wankmüller, F.; Thimmapuram, P.R.; Gallagher, K.G.; Botterud, A. Impact of battery degradation on energy arbitrage revenue of grid-level energy storage. *J. Energy Storage* **2017**, *10*, 56–66. [CrossRef]
35. PJM Valid Source/Sinks for Obligations. Available online: https://www.pjm.com/markets-and-operations/ftr.aspx (accessed on 1 December 2023).
36. PJM Data Miner 2. Available online: https://dataminer2.pjm.com/list (accessed on 1 December 2023).
37. PJM Regulation Requirement Definition. Available online: https://pjm.com/-/media/committees-groups/task-forces/rmdstf/2022/20220322/20220322-item-04-regulation-overview-education.ashx (accessed on 20 February 2024).
38. Kirschen, D.S.; Strbac, G. *Fundamentals of Power System Economics*; John Wiley & Sons: Hoboken, NJ, USA, 2018.
39. PJM RTO Regulation Signal Data. Available online: https://www.pjm.com/-/media/markets-ops/ancillary/rto-regulation-signal-data.ashx (accessed on 20 February 2024).
40. Salles, M.; Huang, J.; Aziz, M.; Hogan, W. Potential arbitrage revenue of energy storage systems in PJM. *Energies* **2017**, *10*, 1100. [CrossRef]
41. Krishnamurthy, D.; Uckun, C.; Zhou, Z.; Thimmapuram, P.R.; Botterud, A. Energy storage arbitrage under day-ahead and real-time price uncertainty. *IEEE Trans. Power Syst.* **2017**, *33*, 84–93. [CrossRef]
42. Vejdan, S.; Grijalva, S. Maximizing the Revenue of Energy Storage Participants in Day-Ahead and Real-Time Markets. In Proceedings of the 2018 Clemson University PSC, Charleston, SC, USA, 4–7 September 2018; pp. 1–6.
43. Mulder, F. Implications of diurnal and seasonal variations in renewable energy generation for large scale energy storage. *J. Renew. Sustain. Energy* **2014**, *6*, 033105. [CrossRef]
44. Annual Motor Carrier Operations Cost Report. Available online: https://trid.trb.org/view/1552714 (accessed on 1 October 2023).
45. PJM Manual 14A: Generation and Transmission Interconnection Process. Available online: https://www.pjm.com/-/media/documents/manuals/archive/m14a/m14av19-generation-and-transmission-interconnection-process-11-01-2016.ashx (accessed on 20 October 2022).
46. PJM Open Access Transmission Tariff. Available online: https://agreements.pjm.com/oatt/4217 (accessed on 1 December 2023).
47. Box, G.E.; Jenkins, G.M.; Reinsel, G.C.; Ljung, G.M. *Time Series Analysis: Forecasting and Control*; John Wiley & Sons: Hoboken, NJ, USA, 2015.
48. Conejo, A.J.; Plazas, M.A.; Espinola, R.; Molina, A.B. Day-ahead electricity price forecasting using the wavelet transform and ARIMA models. *IEEE Trans. Power Syst.* **2005**, *20*, 1035–1042. [CrossRef]
49. Zhao, Z.; Wang, C.; Nokleby, M.; Miller, C.J. Improving short-term electricity price forecasting using day-ahead LMP with ARIMA models. In Proceedings of the 2017 IEEE PES General Meeting, Chicago, IL, USA, 16–20 July 2017; pp. 1–5.
50. Zhao, Z.; Fu, C.; Wang, C.; Miller, C.J. Improvement to the Prediction of Fuel Cost Distributions Using ARIMA Model. In Proceedings of the 2018 IEEE PES General Meeting, Portland, OR, USA, 5–10 August 2018; pp. 1–5.
51. Liao, T.W. Clustering of time series data—A survey. *Pattern Recognit.* **2005**, *38*, 1857–1874. [CrossRef]
52. Kodinariya, T.M.; Makwana, P.R. Review on determining number of Cluster in K-Means Clustering. *Int. J.* **2013**, *1*, 90–95.
53. Ding, C.; He, X. K-means clustering via principal component analysis. In Proceedings of the Twenty-First International Conference on Machine Learning, Banff, AB, Canada, 4–8 July 2004; p. 29.

Disclaimer/Publisher's Note: The statements, opinions and data contained in all publications are solely those of the individual author(s) and contributor(s) and not of MDPI and/or the editor(s). MDPI and/or the editor(s) disclaim responsibility for any injury to people or property resulting from any ideas, methods, instructions or products referred to in the content.